

Supporting Information

Bis[di(4-methoxyphenyl)amino]carbazole-capped Indacenodithiophene as Hole Transport Materials for Highly Efficient Perovskite Solar Cells: the Pronounced Positioning Effect of A Donor Group on the Cell Performance

Yong Hua,^{*a} Song Chen,^b Dongyang Zhang,^a Peng Xu,^a Anxin Sun,^a Yangmei Ou,^a Tai Wu,^a Hanwen Sun,^a Bo Cui,^a and Xunjin Zhu^{*b}

^a Yunnan Key Laboratory for Micro/Nano Materials & Technology, School of Materials Science and Engineering, Yunnan University, Kunming 650091, Yunnan P. R. China.

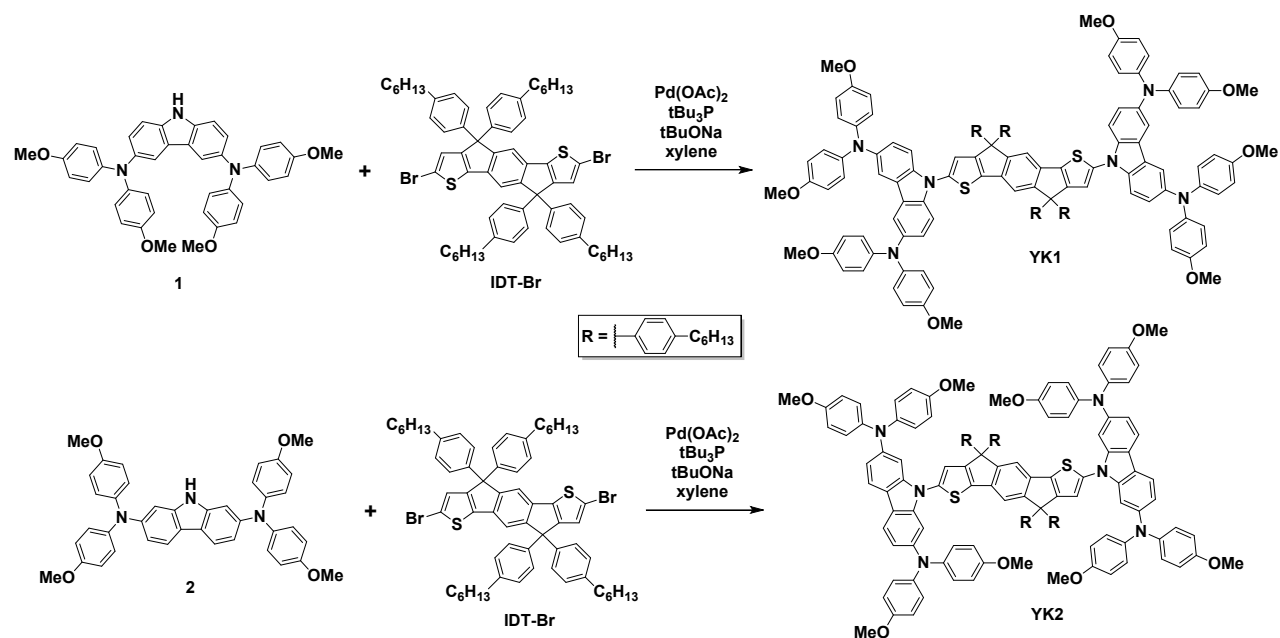
^b Department of Chemistry and Institute of Advanced Materials, Hong Kong Baptist University, Kowloon Tong, Hong Kong, P. R. China.

Corresponding author: huayong@ynu.edu.cn; xjzhu@hkbu.edu.hk;

Experimental Section

Materials and Reagents

Materials were all available commercially and used without further purification if not mentioned specially. The key intermediates *N3,N6-bis*(di-4-anisylamino)-9H-carbazole (**1**),¹ *N2,N7-bis*(di-4-anisylamino)-9H-carbazole (**2**)¹ and 2,7-dibromo-4,4,9-tetrakis(4-hexylphenyl)-4,9-dihydro-s-indaceno[1,2-b:5,6-b']dithiophene² (**IDT-Br**) were synthesized according to the previously reported procedure. The synthetic routes of two HTM **YK1** and **YK2** are outlined in Scheme S1 and the details are depicted. ¹H NMR spectra were recorded using a Bruker Ultrashield 400 Plus NMR spectrometer. High-resolution matrix-assisted laser desorption/ionization time-of-flight (MALDI-TOF) mass spectra were obtained with a Bruker Autoflex MALDI-TOF mass spectrometer.



Scheme S1. The synthesis routes of **YK1** and **YK2**

Synthesis of YK1

A two-necked flask containing IDT2Br (532 mg, 0.5 mmol), compound **4** (683 mg, 1.1 mmol), Pd(OAc)₂ (2.2 mg, 0.01 mmol), sodium *tert*-butoxide (414 mg, 3 mmol), *t*Bu₃P (6.1 mg, 0.03 mmol) and xylene (10 mL) equipped with a magnetic stirrer, a N₂ purge, and a reflux condenser was heated at 120°C for 12 h. The reaction mixture was then poured into water and extracted with CH₂Cl₂ (3 × 50 mL). The combined organic layer was dried with anhydrous Na₂SO₄ and evaporated to dryness. The crude product was purified by silica gel column chromatography with CH₂Cl₂:petroleum ether (1:1, v:v) as eluent affording the compound as a pale yellow solid. ¹H NMR (400 MHz, Benzene-d₆): 7.85 (s, 2 H), 7.81 (d, *J* = 2.0 Hz, 8 H), 7.44 (d, *J* = 8.4 Hz, 4 H), 7.39 (s, 2 H), 7.36 (s, 2 H), 7.27 (d, *J* = 2.0 Hz, 2 H), 7.12 (d, *J* = 5.6 Hz, 16 H), 7.08 (s, 2 H), 7.02 (d, *J* = 8.0 Hz, 8H), 6.73 (d, *J* = 9.2 Hz, 16 H), 3.29 (s, 24 H), 2.44 (t, *J* = 8.0 Hz, 8 H), 1.47 (m, 8 H), 1.20 (m, 24 H), 0.84 (t, *J* = 7.2 Hz, 12 H). (MALDI-TOF, *m/z*) calculated for C₁₄₄H₁₄₀N₆O₈S₂: 2146.0201; found: 2146.0169.

Synthesis of YK2

A two-necked flask containing IDT2Br (532 mg, 0.5 mmol), compound **7** (683 mg, 1.1 mmol), Pd(OAc)₂ (2.2 mg, 0.01 mmol), sodium *tert*-butoxide (414 mg, 3 mmol), *t*Bu₃P (6.1 mg, 0.03 mmol) and xylene (10 mL) equipped with a magnetic stirrer, a N₂ purge, and a reflux condenser was heated at 120°C for 12 h. The reaction mixture was then poured into water and extracted with CH₂Cl₂ (3 × 50 mL). The combined organic layer was dried with anhydrous Na₂SO₄ and evaporated to dryness. The crude product was purified by silica gel column chromatography with CH₂Cl₂:petroleum ether (1:1, v:v) as eluent affording the compound as a pale yellow solid. ¹H NMR (400 MHz, Benzene-d₆): 7.84 (d, *J* = 8.4 Hz, 4 H), 7.71 (d, *J* = 2.0 Hz, 4 H), 7.61 (s, 2 H),

7.21 (m, 28 H), 7.07 (d, $J = 8.4$ Hz, 8 H), 6.99 (s, 2 H), 6.79 (dd, $J_1 = 2.0$ Hz, $J_2 = 6.8$ Hz, 16 H), 3.38 (s, 24 H), 2.68 (t, $J = 8.0$ Hz, 8 H), 1.73 (m, 8 H), 1.41 (m, 8 H), 1.33 (m, 16 H), 0.95 (t, $J = 6.8$ Hz, 12 H). (MALDI-TOF, m/z) calculated for $C_{144}H_{140}N_6O_8S_2$: 2146.0201; found: 2146.3087. 2146.0201; found: 2146.3087.

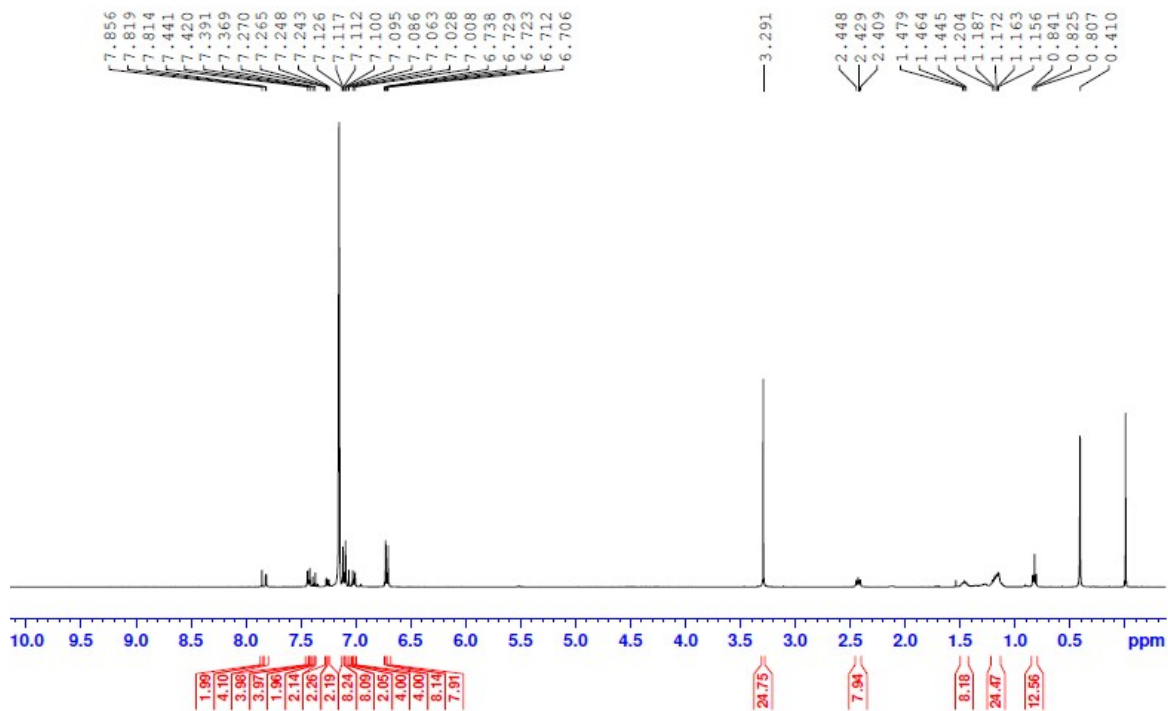


Figure S1. 1H NMR spectra of YK1

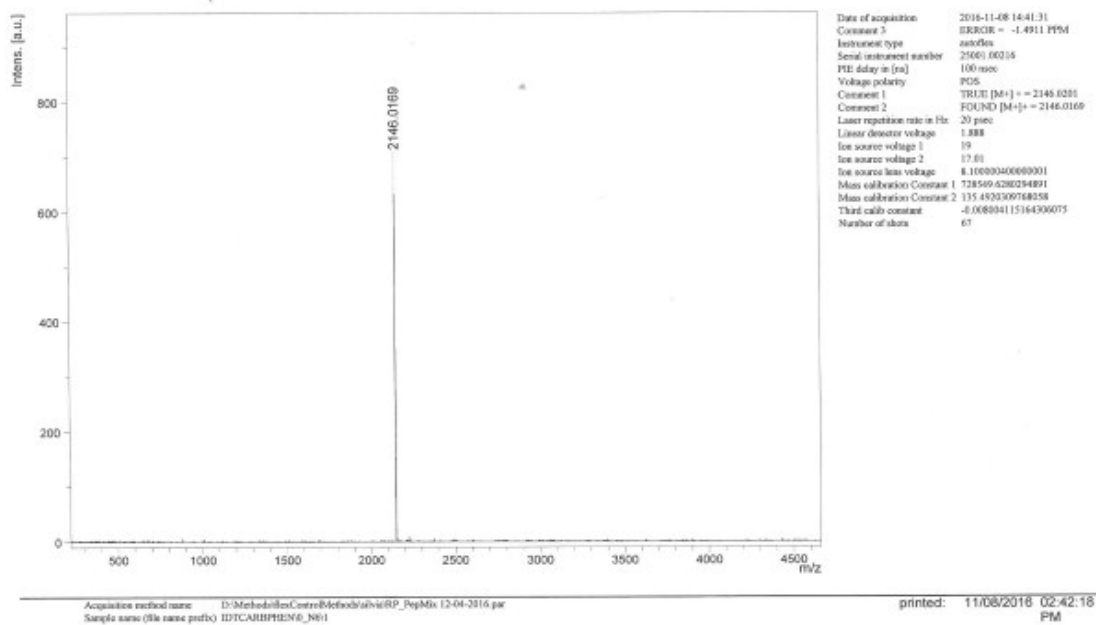


Figure S2. Mass spectrum of YK1

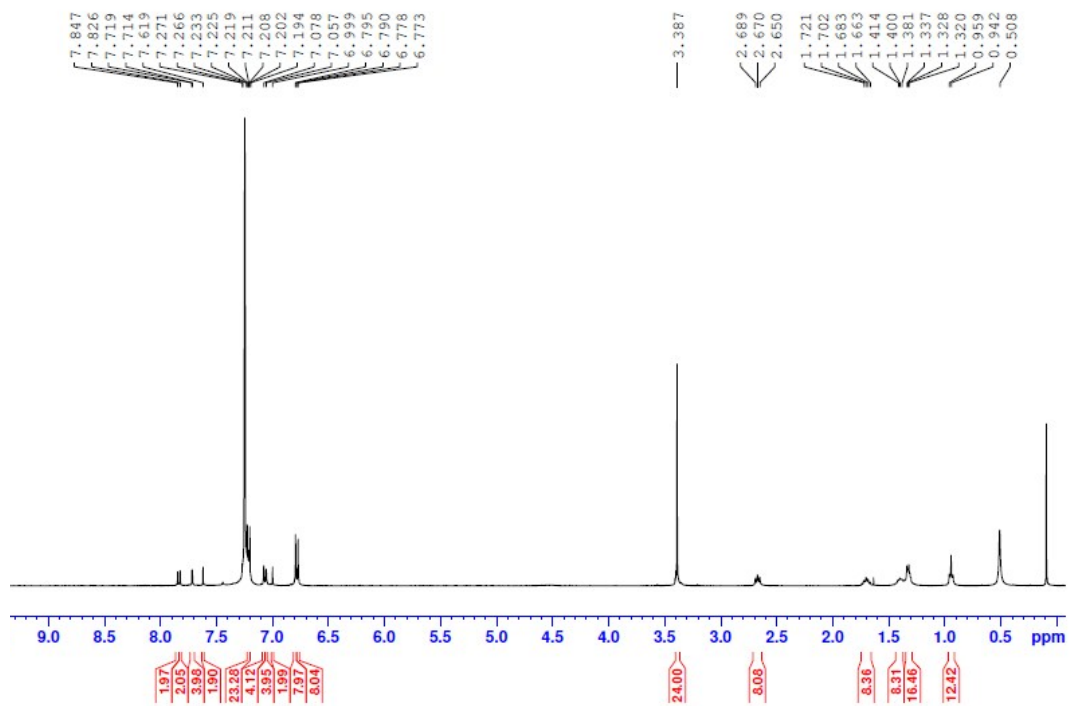


Figure S3. ^1H NMR spectra of YK2

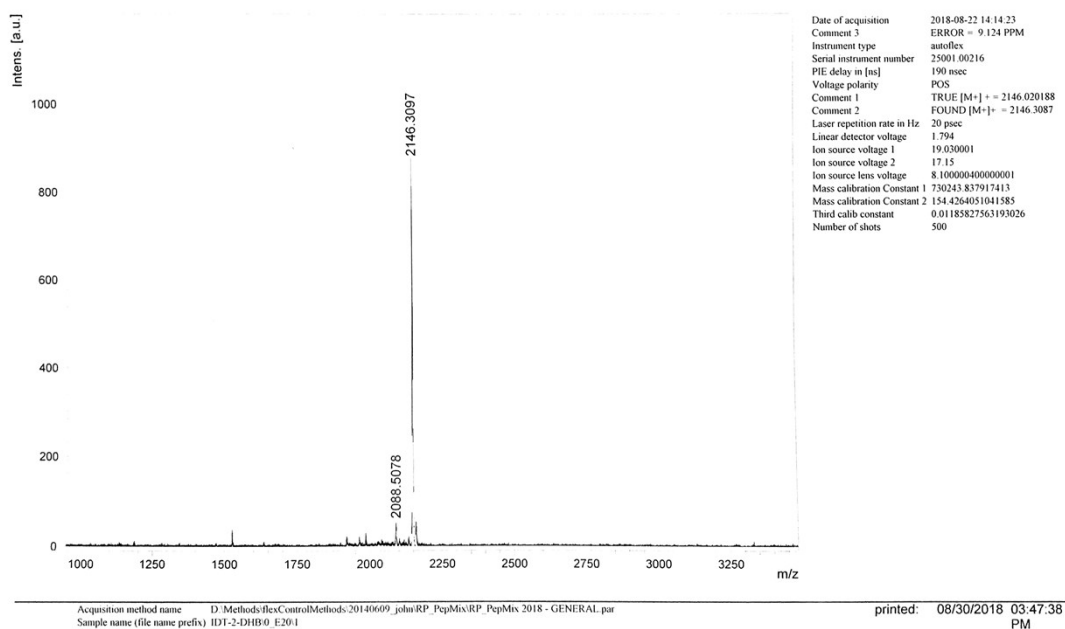


Figure S4. Mass spectrum of YK2

Table S1: A summary of the detail performance parameters of the reported highly efficient small-organic molecules HTMs with PCEs >19%.

HTM	Device structure	J_{SC} (mA cm ⁻²)	V_{OC} (V)	FF (%)	PCE (%)	Ref
FDT	FTO/compactTiO ₂ /mpTiO ₂ /[(FAPbI ₃) _{0.85} (MAPbBr ₃) _{0.15}]/HTM/Au	22.7	1.14	76	20.2	3
X59	FTO/compact-TiO ₂ /mp-TiO ₂ / [(FAPbI ₃) _{0.85} (MAPbBr ₃) _{0.15}]/HTM/Au	23.4	1.13	73	19.8	4
DDOF	FTO/compact-TiO ₂ /mp-TiO ₂ / (FAPbI ₃) _{0.85} (MAPbBr ₃) _{0.15} /HTM/Au	22.37	1.10	79	19.4	5
H12	FTO/compact-TiO ₂ /mp-TiO ₂ / (FAPbI ₃) _{0.85} (MAPbBr ₃) _{0.15} /HTM/Au	24.2	1.15	71	19.8	6
V862	FTO/compact-TiO ₂ /mp-TiO ₂ / (FAPbI ₃) _{0.85} (MAPbBr ₃) _{0.15} /HTM/Au	22.5	1.14	77	19.9	7
KR321	FTO/compact-TiO ₂ /mp-TiO ₂ / (FAPbI ₃) _{0.85} (MAPbBr ₃) _{0.15} /HTM/Au	21.70	1.13	78	19.0	8
IDIDF	FTO/compact-TiO ₂ /mp-TiO ₂ / [FAPbI ₃] _{0.92} [MAPbBr ₃] _{0.08} /HTM/Au	23.55	1.05	77	19.0	9
Z26	FTO/compact-TiO ₂ /mp-TiO ₂ / (FAPbI ₃) _{0.85} (MAPbBr ₃) _{0.15} /HTM/Au	23.59	1.13	75	20.1	10

X55	FTO/compact-TiO ₂ /mp-TiO ₂ / (FAPbI ₃) _{0.85} (MAPbBr ₃) _{0.15} /HTM/Au	23.4	1.15	77	20.8	11
X26	FTO/compact-TiO ₂ /mp-TiO ₂ / (FAPbI ₃) _{0.85} (MAPbBr ₃) _{0.15} /HTM/Au	24.3	1.11	75	20.2	12
SiOMeTPA	ITO/HTL/MAPbI ₃ /PCBM/Al	23.08	1.07	72	19.1	13
Co(II)P/ Co(III)P	FTO/compact-TiO ₂ /mp-TiO ₂ / (CsFAMA)Pb(BrI) ₃ /HTM/Au	23.62	1.13	77	20.5	14
SCZF-5	FTO/compact-TiO ₂ /mp-TiO ₂ / MAPbI ₃ /HTM/MoO ₃ /Ag	24.40	1.11	74	20.1	15
G2	FTO/compact-TiO ₂ /mp-TiO ₂ / (FAPbI ₃) _{0.85} (MAPbBr ₃) _{0.15} /HTM/Au	23.52	1.13	76	20.2	16
OMeTATPyr	FTO/compact-TiO ₂ /mp-TiO ₂ / Cs _{0.05} FA _{0.81} MA _{0.14} PbI _{2.55} Br _{0.45} /HTM/Au	23.3	1.10	81	20.6	17
EDOT-Amide- TPA	FTO/compact-TiO ₂ /mp-TiO ₂ / MAPbI ₃ /HTM/Au	22.7	1.16	77	20.3	18
YK1	FTO/compact-TiO ₂ /mp-TiO ₂ / (FAPbI ₃) _{0.85} (MAPbBr ₃) _{0.15} /HTM/Au	23.55	1.11	77	20.13	This work

Mobility Measurements

Hole mobility was measured by using the SCLC method, which can be described by the following equation

$$J = \frac{9}{8} \mu \epsilon_0 \epsilon_r \frac{V^2}{d^3}$$

where J is the current density, μ is the hole mobility, ϵ_0 is the vacuum permittivity (8.85×10^{-12} F/m), ϵ_r is the dielectric constant of the material (normally taken to approach 3 for OSs), V is the applied bias, and d is the film thickness.

The detailed device fabrication follows: Indium Tin Oxide (ITO) coated glass substrates (Pilkington TEC15) were patterned by etching with zinc powder and 2 M hydrochloric acid. The substrates were carefully cleaned in ultrasonic baths of detergents, deionized water, acetone and ethanol successively. The remaining organic residues were removed with 10 min by airbrush. A 40 nm thick PEDOT: PSS layer was spin-coated onto the substrates, which were then annealed at

120 °C for 30 min in air. The substrates were then transferred into a glovebox for further fabrication steps. The HTMs were dissolved in anhydrous chlorobenzene. Here the concentration of YK1/YK2 is 40 mg mL⁻¹ in chlorobenzene with addition of 8 μL Li-TFSI (520 mg Li-TFSI in 1 mL acetonitrile), 14 μL tert-butylpyridine (*t*BP) and 1 μL FK209 solution (2 M FK209 in acetonitrile). This HTMs solution was spin-coated at 4000 rpm to yield films. The thicknesses of the films are measured by using a Dektak 6M profilometer. 80 nm of gold was then evaporated onto the active layer under high vacuum (less than 10⁻⁶ mbar). *J-V* characteristics of the devices have been measured with a Keithley 2400 Source-Measure unit, interfaced with a computer. Device characterization was carried out in air.



Figure S5. Schematic illustration of the mobility device.

Fabrication of (FAPbI₃)_{0.85}(MAPbBr₃)_{0.15} perovskite solar cells

The fluorine-doped SnO₂ (FTO, 15 Ω-square) substrates were etched with zinc powder and HCl acid (concentration 4 M) to form the desired electrode pattern. The substrates were cleaned in an ultrasonic bath for half an hour in the following order: deionized water, acetone and ethanol. A compact layer of TiO₂, intended to block the recombination current at the FTO support, was prepared on cleaned FTO substrate by spray pyrolysis of solution (0.2M titanium isopropoxide and 2M acetylacetone in isopropanol). Afterwards, a layer of mesoporous TiO₂ particles were spin-coated on the FTO glass with a thickness of 200 nm. The perovskite films were deposited from a precursor solution containing FAI (1 M), PbI₂ (1.1 M), MABr (0.2 M) and PbBr₂ (0.2 M)

in anhydrous DMF: DMSO=4:1 (v/v). The perovskite solution was spin-coated in a two-step program; first at 1000rpm for 10 s and then at 4000 rpm for 30 s. During the second step, 100 μ L of chlorobenzene were poured on the spinning substrate 15s prior to the end of the program. The substrates were then annealed at 100 $^{\circ}$ C for 1 h in a nitrogen filled glove box. Then, the YK1, YK2 and Spiro-OMeTAD/chlorobenzene solution were spin-coated at 4000 rpm for 30 s. For Spiro-OMeTAD HTMs, Spiro-OMeTAD in chlorobenzene solution (80 mg mL⁻¹) was employed with the additives containing 17.5 μ L Li-TFSI/acetonitrile (520 mg mL⁻¹), 28.8 μ L TBP and 2 μ L FK209 solution (2 M FK209 in acetonitrile). For YK HTMs, YK1/YK2 in chlorobenzene solution (40 mg mL⁻¹) were prepared by mixing the additives containing 8 μ L Li-TFSI/acetonitrile (520 mg mL⁻¹), 14 μ L TBP and 1 μ L FK209 solution (2 M FK209 in acetonitrile). As a last step 80 nm of gold top electrode were thermally evaporated under high vacuum. Current-voltage characteristics were measured under 100 mW/cm² (AM 1.5G illumination) using a Newport solar simulator (model 91160) and a Keithley 2400 source/meter. A certified reference solar cell (Fraunhofer ISE) was used to calibrate the light source for an intensity of 100 mW/cm². Incident photon-to-current conversion efficiency (IPCE) spectra were recorded using a computer-controlled setup consisting of a Xenon light source (Spectral Products ASB-XE-175), a monochromator (Spectra Products CM110), and a potentiostat (LabJack U6 DAQ board), calibrated by a certified reference solar cell (Fraunhofer ISE). Electron lifetime measurements were performed using a white LED (Luxeon Star 1W) as the light source. The photocurrent decay was determined by monitoring photocurrent transients by applying a small square-wave modulation to the base light intensity. The voltage scan rate was 10mV s⁻¹ and no device preconditioning was applied before starting the measurement, such as light soaking or

forward voltage bias applied for long time. The cells were masked with a black metal mask limiting the active area to 0.09 cm² and reducing the influence of the scattered light.

- (1) Y. Shi, K. Hou, Y. Wang, K. Wang, H. Ren, M. Peng, F. Chen, S. Zheng, *J. Mater. Chem. A*, 2016, **4**, 5415.
- (2) M. Wang, X. W. Hu, L. Q. Liu, C. H. Duan, P. Liu, L. Ying, F. Huang, Y. Cao, *Macromolecules*, 2013, **46**, 3950.
- (3) M. Saliba, S. Orlandi, T. Matsui, S. Aghazada, M. Cavazzini, J.-P. Correa-Baena, P. Gao, R. Scopelliti, E. Mosconi, K.-H. Dahmen, F. De Angelis, A. Abate, A. Hagfeldt, G. Pozzi, M. Graetzel and M. K. Nazeeruddin, *Nat. Energy*, 2016, **1**, 15017.
- (4) D. Bi, B. Xu, P. Gao, L. Sun, M. Grätzel and A. Hagfeldt, *Nano Energy*, 2016, **23**, 138.
- (5) K. Rakstys, S. Paek, M. Sohail, P. Gao, K. Taek Cho, P. Gratia, Y. Lee, K. H. Dahmen and M. K. Nazeeruddin, *J. Mater. Chem. A*, 2016, **4**, 18259.
- (6) J. Zhang, Y. Hua, B. Xu, L. Yang, P. Liu, M. B. Johansson, N. Vlachopoulos, L. Kloo, G. Boschloo, E. M. J. Johansson, L. Sun, A. Hagfeldt, *Adv. Energy Mater*, 2016, **6**, 1601062.
- (7) T. Malinauskas, M. Saliba, T. Matsui, M. Daskeviciene, S. Urnikaite, P. Gratia, R. Send, H. Wonneberger, I. Bruder, M. Grätzel, V. Getautis, M. K. Nazeeruddin, *Energy Environ. Sci*, 2016, **9**, 1681.
- (8) K. Rakstys, S. Paek, P. Gao, P. Gratia, T. Marszalek, G. Grancini, K. T. Cho, K. Genevicius, V. Jankauskas, W. Pisula, M. K. Nazeeruddin, *J. Mater. Chem. A*, 2017, **5**, 7811.
- (9) I. Cho, N. J. Jeon, O. K. Kwon, D. W. Kim, E. H. Jung, J. H. Noh, J. Seo, S. I. Seok, S. Y. Park, *Chem. Sci*, 2017, **8**, 734.
- (10) F. Zhang, Z. Wang, H. Zhu, N. Pellet, J. Luo, C. Yi, X. Liu, H. Liu, S. Wang, X. Li, Y. Xiao, S. M. Zakeeruddin, D. Bi, M. Grätzel, *Nano Energy*, 2017, **41**, 469.
- (11) B. Xu, J. Zhang, Y. Hua, P. Liu, L. Wang, C. Ruan, Y. Li, G. Boschloo, E. M. J. Johansson, L. Kloo, A. Hagfeldt, A. K.-Y. Jen, L. Sun, *Chem*, 2017, **2**, 676.
- (12) J. B. Zhang, B. Xu, L. Yang, C. Q. Ruan, L. Q. Wang, P. Liu, W. Zhang, N. Vlachopoulos, L. Kloo, G. Boschloo, L. Sun, A. Hagfeldt, E. M. J. Johansson, *Adv. Energy Mater*, 2017, 1701209
- (13) R. Xue, M. Zhang, G. Xu, J. Zhang, W. Chen, H. Chen, M. Yang, C. Cui, Y. Li, Y. Li, *J. Mater. Chem. A*, 2018, **6**, 404.

- (14) J. Cao, X. D. Lv, P. Zhang, T. T Chuong, B. H. Wu, X. X. Feng, C. F. Shan, J. C. Liu, Y. Tang, *Adv. Mater.* 2018, **30**, 1800568.
- (15) X. D. Zhu, X. J. Ma, Y. K. Wang, Y. Li, C. H. Gao, Z. K. Wang, Z. Q. Jiang, L. S. Liao, *Adv. Funct. Mater.* 2018, 1807094.
- (16) K. Gao, B. Xu, C. S. Hong, X. L. Shi, H. B. Liu, X. S. Li, L. H. Xie, A. K.Y. Jen, *Adv. Energy Mater.* 2018, **8**, 1800809.
- (17) Q. Q. Ge, J.Y. Shao, J. Ding, L.Y. Deng, W. K. Zhou, Y. X. Chen, J. Y. Ma, L. J. Wan, J. N. Yao, J. S. Hu, Y. W. Zhong, *Angew Chem*, 2018, **57**, 10959.
- (18) M. L. Petrus, K. Schutt, M. T. Sirtl, E. M. Hutter, A. C. Closs, J. M. Ball, J. C. Bijleveld, A. Petrozza, T. Bein, T. J. Dingemans, T. J. Savenije, H. Snaith, P. Docampo, *Adv. Energy Mater.* 2018, **8**, 1801605.